

# A Test Method and Model to Determine The Thermal Initiation Properties of An Energetic Material In A Low Pressure Long Duration Event

J.G. Glenn, Dr. Joseph C. Foster  
Air Force Research Laboratory  
Eglin AFB FL

Mr. Mike Gunger, Dr. Jin Yao  
General Dynamics/Ordnance and Tactical Systems  
Niceville, FL

Dr. Alain Beliveau  
Applied Research Associates,  
2004 Lewis Turner Blvd FWB, FL

## **Abstract**

A combined experimental and analytical program to develop insight into both the mechanical and thermal response of energetic materials under low pressure, long impulse loading has been under development by AFRL/MNME. The mechanical aspects of the work have been previously reported. This paper will address the continuing effort with regard to thermal effects generated by friction. The work reported herein, while applicable to the general class of energetic materials, is intended to provide insight into the thermal response of explosives in hazard classes 1.1 to 1.6 under loading conditions in the millisecond range.

## **Introduction**

A significant body of work has been produced with regard to shock initiation of energetic materials. Typically, most of the published data, primarily Hugoniot data, have been generated in the region of interest with regard to high pressure, high rate loading generally referred to as SDT (Shock-to-Detonation Transition). However, numerous conditions exist under which an energetic material is subjected to loads and load rates well below that of SDT but which still results in an energetic response. Field<sup>1</sup> lists initiation mechanisms most likely to manifest under mechanical deformation as:

1. Adiabatic compression of trapped gas spaces
2. Viscous heating of material rapidly extruded between impacting surfaces or grains.
3. Friction between the impacting surfaces, the explosive crystals and/or grit particles in the explosive layer.
4. Localized adiabatic shear of the material during mechanical failure.

Field provides further references for each of the mechanisms in the paper cited. Chaudhri<sup>2</sup> has investigated each of these mechanisms on a crystal basis. His findings indicate that intercrystalline

friction is a dominant mechanism under mechanical deformation. The effect of various binders to either enhance or minimize these effects is further explored in Reference 3 particularly with regard to the generation of free surfaces. In general, low stress; low strain rate events were dominated by cracks forming around the crystals as opposed to cracking within the crystal itself. However, data previously presented from the Piston Test<sup>4</sup> indicated substantial intergranular shear, hence the formation of additional free surfaces due to the relatively high pressures imposed (~1-5 kbars). It is expected that the formation of these surfaces will enhance the susceptibility of the explosive to a thermal event. The data suggests that friction is an efficient mechanism with regard to both heat generation as well as heat transfer due to the intimate surface contact. As a result, we have focused on friction as a dominant mechanism in this paper.

The work presented herein will be divided between the experimental and

analytical efforts. We are calling these tests and simulations "The Explosive Survivability Protocol". Recent data from the Intense Pressure and Friction Test will be presented along with the approach to measuring both the bonding strength of an explosive to a surface and the derivation of friction coefficients.

### Experimental

This section will describe the development of the experimental methods used to characterize both the mechanical and thermal response of explosives. As the mechanical characterization has been previously reported, only a summary of the method will be given here. The piston test and sample plot are shown in Figure 1. Based upon the load applied, the test gives a pressure versus volume change for the explosive. This information is then used to develop an appropriate Low Pressure Equation of State (LPEOS) model. Typically, this results in either a low-pressure Hugoniot representation or a crush-up model

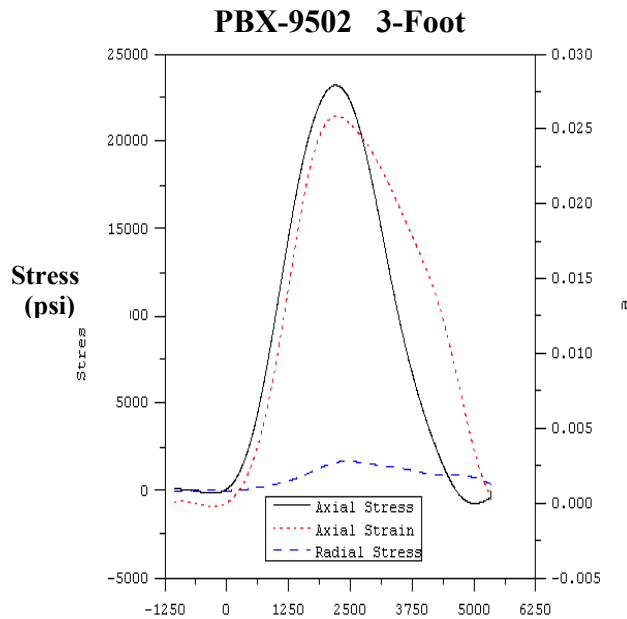


Figure 1. Piston Test and Sample Plot

### **Breakaway Strength Tests**

A need arose to determine the amount of pressure (strength) required to move the explosive liner system. Previous experimental data had suggested that most energetic material was essentially free to move on boundaries, however, none of the data was conclusive. As a result, a test was devised to determine both the breakaway strength and the propensity for shear in the bulk. For these experiments steel cylinders were lined with asphaltic hot melt (AHM) liner material, cured and then loaded with two different explosive simulants. The explosive simulants were 1.) Cast Cure using Hydroxy-Terminated Polybutadiene (HTPB) as the binder system and 2.) Melt Cast (Filler E) using a wax-based material as binder. The Cast Cure has a rubbery feel to it and the Melt Cast is hard and brittle. These tests were conducted using an Instron machine applying a compressive load at 50 inches/minute. This behavior is very important in relation to the friction surface that the explosive will be exposed to during the Low Pressure Long Duration event. Figures 2 & 3 show the post test samples and how the explosive simulant/liner responded to the applied load. The Cast Cure system made a clean break from the liner. The Melt Cast plugged and some of the material broke free under a much greater pressure.

Data from the test showed that the Melt Cast System has good bond strength to the liner as well as the liner to the casewall. The Cast Cure system has very weak bond strength to the liner. The breakaway test results showed it had a bond strength of 50 psi versus 350 psi

or the melt cast, or about 1/7 of the bond strength.

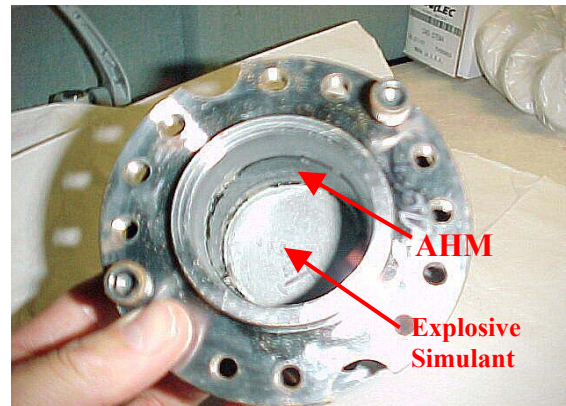


Figure 2. Cast cure system showing breakaway from simulant/liner



Figure 3. Melt cast system showing the plugging and the breakaway

### **Intense Pressure and Friction Test**

The Intense Pressure and Friction Test (IPFT) was developed to complete the suite of tests that make up the Explosive Survivability Protocol. This test is designed to subject the explosive to a Low Pressure Long Duration event in a highly controlled instrumented environment. The test sample is 50.8 mm diameter by 50.8 mm long. The IPFT cylinder is 36 cm long and has an inside diameter of 50.8 mm.

There are two IPFT cylinders that are used, they vary only by the surface finish on the inside. We set out to create an environment that was highly controllable for the explosive. A series of tests were conducted to determine the coefficient of sliding friction, as a function of various surface finishes. It was determined that the surface finish that was most similar to the surface finish of the cured AHM material was 60 reams (rms). Therefore the 60 rms finish was machined onto the inside surface of the IPFT cylinder and the test was conducted without the AHM liner material. Then a surface finish of 500 rms was used to generate a more severe environment for the explosive. The explosive sample is placed inside the cylinder with a 50.8 mm diameter by 12.7 mm thick disc of inert material that has the same binder system as the explosive on both sides of the explosive. Two steel discs 50.8 mm diameter by 12.7 mm thick are placed on the outside of the inert material. The whole system as shown in Figure 4 is slid inside the steel IPFT cylinder at a given pressure and velocity. The inputs for determining the needed pressure and velocity are determined by hydrocode modeling.

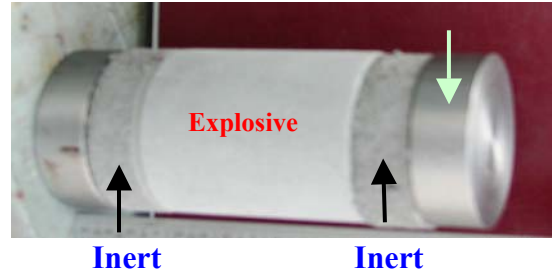


Figure 4. Explosive/inert/steel discs

Once the explosive system has been inserted into the IPFT cylinder, input and output pistons are inserted. An aluminum honeycomb (for pressure regulation) material is placed between the output piston and a rigid mounted steel plate. A steel billet is fired out of a black powder gun down a rail into the input piston. Fiber optics are used to measure the velocity of the billet before impact. Accelerometers are placed on the input and output pistons for measuring the velocity of the pistons, which is the velocity of the explosive sample. Finally three ballistic pressure transducers are placed on the side (radial measurement) of the IPFT cylinder. These pressure transducers give a complete history of the pressure induced into the sample and any resulting reaction. Figure 5 shows the test cylinder with instrumentation attached.

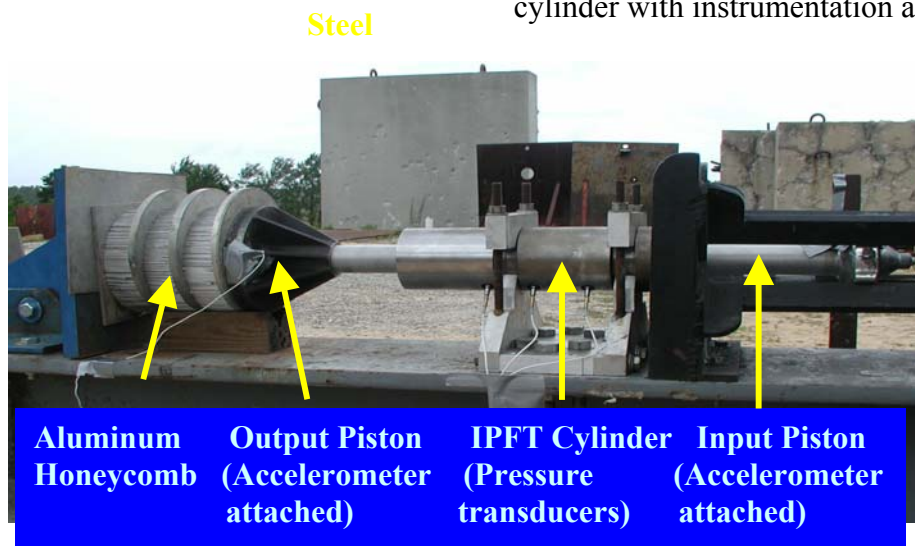


Figure 5. IPFT Cylinder with instrumentation attached

A series of tests were conducted with a cast cure explosive. The tests consisted of: all inert materials, live explosive with 60 rms surface finish and live explosive 500 rms surface finish. The input conditions that were held constant were; anvil weight 11.35 kg, anvil velocity 76 m/s, aluminum honeycomb material is 15.24 cm thick

### **Results**

#### **Test Case #1 - 60 rms finish/all inert materials**

The highest measured radial pressure was 120 ksi and the peak sliding velocity was 46 m/s. The input piston was stuck inside the IPFT cylinder and had to be physically removed.

#### **Test Case #2 - 60 rms finish/inert-live explosive-inert**

The highest measured radial pressure was 124 ksi and the peak sliding velocity was 46 m/s. The difference between the inert material and this test was the following: the input was blown out of the IPFT cylinder and showed signs of

blackening from a reaction. A small bit of smoke came out of the barrel after the input piston was blown out. The explosive was totally recovered. It appears that some type of deflagration reaction occurred.

#### **Test Case #3 - 500 rms finish/inert-live explosive-inert**

The highest measured radial pressure was 126 ksi and the peak sliding velocity was 46 m/s. Figure 6 shows the high-speed video image of the very violent reaction that occurred. After the input piston was blown out, a significant amount of explosive was blown out of the IPFT cylinder and commenced to burn. Only 46 grams out of 150 grams were recovered. However, the radial pressure is very similar to the first two cases. The timing of the reaction is still under study.

Data from the test is tabulated in Table 1. As can be seen, under reasonably similar forcing functions, the reaction of the energetic was significantly more violent for the 500 rms finish.



Figure 6. Violent Reaction Cast Cure Explosive

TABLE I

Test Material	Surface Finish	Input piston Velocity	Output Piston Velocity	Radial Pressure			Reaction
				P1	P2	P3	
Simulant	60 rms	*NA	NA	Data lost			None
Simulant	60 rms	53 m/s	46 m/s	124ksi	97ksi	15ksi	None
Explosive Cast Cure	60 rms	NA	NA	120ksi	39ksi	10ksi	Mild
Explosive Cast Cure	60 rms	46 m/s	46 m/s	123 ksi	59 ksi	8ksi	Mild
Explosive Cast Cure	500 rms	Data Lost	Data Lost	124 ksi	100 ksi	2.5 ksi	Violent
Explosive Cast Cure	500 rms	46 m/s	46 m/s	126 ksi	67 ksi	25 ksi	Violent
Explosive Cast Cure	500 rms	NA	NA	139 ksi	80 ksi	25 ksi	Violent

\*NA-Data is not available yet.

## MODELING

The objective of the Survivability Protocol is to develop a set of tools which will reduce the likelihood of a premature energetic event for energetic materials subjected to low pressure, long impulse loading. For our application, this type of loading results in bulk motion between the energetic material and a container or the development of internal shear forces, which, in turn, induce inter/intra granular motion. The result of this motion is the generation of heat, which may be sufficient to cause a thermal reaction. Previous efforts have focused on developing a capability to determine the constitutive response of

the bulk energetic. Based upon this information, models and parameters were developed which allowed the bulk motion of the energetic to be modeled under various load conditions. This, in turn, provides the information necessary to determine the potential for the development of a thermal threat. This section will describe the modeling approaches under development as well as the incorporation of a friction model in the MLSPH code. As constitutive modeling has been previously reported, this section will present approaches to modeling the thermal threat.

The general heat equation is written as

$$\nabla^2 T + q'''/k = 1/\alpha(\partial T/\partial t) \quad (1)$$

where

$\nabla^2$  is the Laplacian operator  
 $q'''$  is the heat generated on a volume basis ( $J/m^3$ )  
 $T$  is the temperature (K)  
 $k$  is the thermal conductivity ( $W/m \cdot K$ )  
 $\alpha$  is the thermal diffusivity ( $m^2/sec$ )

The rate of heat generated by friction can be expressed as<sup>5</sup>

$$q' = \mu \tau v \quad (2)$$

where

$q'$  is the rate of heat generation ( $J/sec$ )  
 $\mu$  is the coefficient of friction  
 $\tau$  is the tangential component of traction (Mpa)  
 $v$  is the sliding velocity (m/sec)

Assuming one-dimensional planar flow, equation (1) can be rewritten as

$$\rho C_v dT/dt = k T_{xx} + \rho(dQ/dt) \quad (3)$$

where  $Q$  is the rate of heat increase on a mass basis,  $\rho$  is the density and  $C_v$  is the specific heat.  $Q$  is the sum of both chemical and mechanical heat production given as

$$dQ/dt = Q_r v e^{-E/RT} + q'/m \quad (4)$$

where  $Q_r v$  is the pre-exponential multiplication factor in Arrhenius kinetics,  $E$  is the Arrhenius energy barrier constant and  $R$  the universal gas constant.

These expressions form the basis for the inclusion of thermal effects in the

MLSPH code to be discussed later.

The analytic expression for the temperature increase due to the rubbing of two surfaces over a circle of radius  $a$ , developed by Bowden and Yoffe<sup>6</sup>, is given as

$$\Delta T = F_f v / 8ak \quad (5)$$

Where  $F_f$  is the force due to friction and  $v$  is the sliding velocity. Clearly, the temperature rise for most problems of interest is significant when steady state conditions are assumed. A modification was made by Coffey et. al. to establish a microstructural basis for the development of heat associated with friction by incorporating a critical microstructural stress intensity factor ( $k_s = \tau l^{1/2}$ ) where  $l$  is the crystal size and  $\tau$  is the shear stress. Replacing the friction force with the shear stress and the appropriate area, the following equation was developed

$$\Delta T = \pi k_s l^{1/2} v / 16k$$

This equation requires that data for the cleavage factor,  $k_s$ , be developed. Previous micrographs have indicated significant shearing of crystals under the loading developed in the IPTF. The development of the temperature rise dependence on shear stress is important because it allows the incorporation of initiation mechanisms into existing reactive flow models such as Greek Fire<sup>7</sup>.

### **The SPH model of interface friction:**

The IPFT was developed to subject energetic materials to an environment characterized by low pressure, long impulse loading. However, by itself, the test does not provide insight into the

initiation mechanisms that may manifest under these conditions. The incorporation of the Greek Fire reactive flow model into an SPH formulation allows explicit treatment of multi phase flow while preserving material interfaces. The development of the Moving Least Squares Smooth Particle Hydrodynamic (MLS<sup>2</sup>SPH) formulation follows that of Dilts<sup>8,9</sup>. The formulation has been extended by incorporating a rezone technique that has the effect of removing tensile instabilities.

What follows is a description of the approach taken to model the effects of friction under pressure loading. The response of energetics to the environment developed in the IPFT will be used to validate/extend the current model. It should be noted that this is a work in progress. As a result, this section will describe the results obtained so far. A significant body of work remains to accomplish the goals of the program.

GD-OTS has developed an upgraded SPH simulator to solve general problems in material interactions. SPH (smooth-particle-hydrodynamics) treats the dynamic system as sets of spatial interpolation points (particles). Each of the particles is associated with a definite mass, has its own momentum, energy, stress and strain. The motion of such a particle is governed with an equation system equivalent to the conservation laws in continuum mechanics. Therefore one is able to trace the motion of all the particles in the system so that the complete description of the motion of the whole system is achieved. This numerical tool can easily be used to model friction between material interfaces.

The motion of a certain particle  $n$  is only determined by nearby particles. These particles are called the *neighbors* of the particle  $n$ . In SPH it is essential to find these neighbors for interpolants in the system. The contribution from each neighbor of particle  $n$  then is summed up to complete the source terms in SPH governing the equations of motion of particle  $n$ . For a proper treatment of *boundary conditions*, the *boundary* particles need to be detected correctly.

The following describes the SPH modeling of friction that is being used in this work.

We assume materials **A** and **B** are in contact and their *boundary* particles are correctly identified and well ordered. For a *boundary* particle  $n_a$  in material **A**, it is considered on the interface between material **A** and material **B** if there is at least one particle  $n_b$  of material **B** which is a neighbor of  $n_a$ . We may calculate the normal vector  $\hat{n}$  and the tangential vector  $\hat{t}$  at particle  $n_a$  given the positions of  $n_a$  and its **B** neighbors. The geometric understanding of the *interface* is a spatial curve (2D) that has equal minimum distance from both **A** and **B**. The normal stress at particle  $n_a$  is calculated with  $\sigma_{nn} = \hat{n} \cdot \vec{\sigma} \cdot \hat{n}$ , where  $\vec{\sigma}$  is the total stress of  $n_a$ .

We define the friction contribution to the stress of an *interface* particle by the term  $\vec{\sigma}_f$ , where

$$\vec{\sigma}_f = \mu \sigma_{nn} (\hat{n} \otimes \hat{t} + \hat{t} \otimes \hat{n}) \quad \text{where}$$

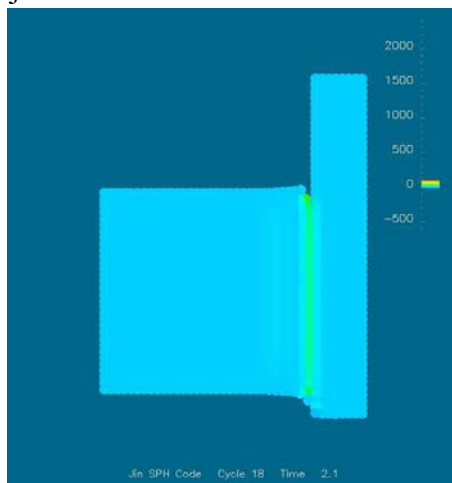
$\mu$  is the coefficient of friction. This choice provides the shear stress applied to the interface particle from friction. It is easy to see that

$\hat{n} \cdot \vec{\sigma}_f \cdot \hat{t} = \hat{t} \cdot \vec{\sigma}_f \cdot \hat{n} = \mu \sigma_{nn}$  and  
 $\hat{n} \cdot \vec{\sigma}_f \cdot \hat{n} = \hat{t} \cdot \vec{\sigma}_f \cdot \hat{t} = 0$ , therefore it is a  
 pure shear and equal to the friction  
 applied to  $n_a$ . When  $\sigma_{nn}$  is positive, there  
 is no friction applied.

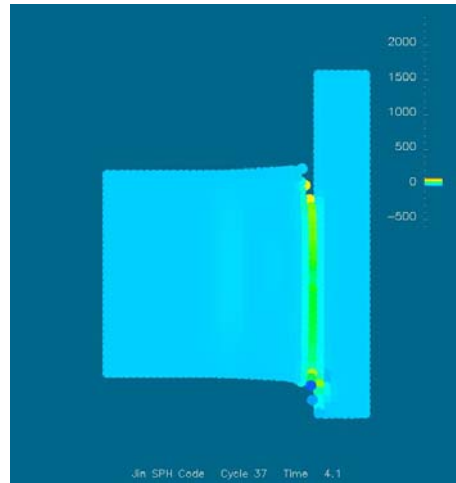
The total stress of the interface particle  
 $n_a$  then is adjusted to  $\vec{\sigma} + \text{sgn}(\delta v_t) \vec{\sigma}_f$ ,  
 where  $(\delta v_t)$  is the relative tangential  
 velocity between particle  $n_a$  and the  
 point on the *interface* coincident with  
 $n_a$ 's projection on the interface. This

projection point can be defined with the  
 positions of  $n_a$  and its neighbors. When  
 $(\delta v_t)$  is zero or the normal stress is  
 positive, we turn off the friction by  
 setting  $\mu = 0$ .  $\mu$  is always set to zero for  
 particles not on the interface.

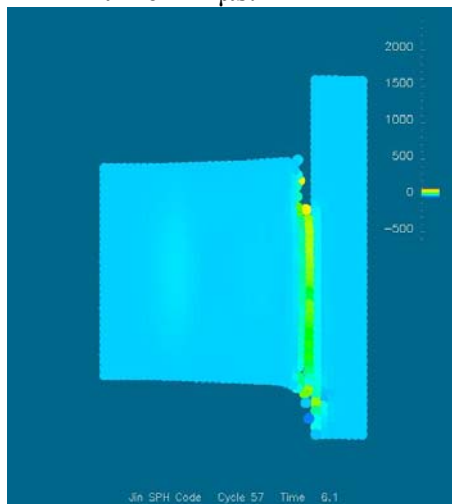
In the governing equations of particle  $n_a$   
 , only the stress term is changed. The  
 conservation laws do not change. The  
 heat generated by friction is  
 automatically included.



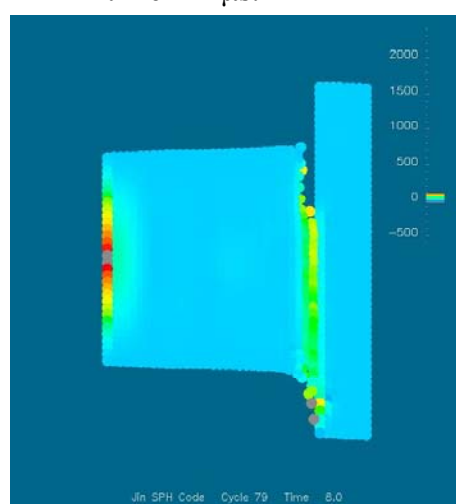
time = 2 μs.



time = 4 μs.



time = 6 μs.



time = 8 μs.

Figure 7. MLSPH Model of the Interaction of a Friction Surface

Figure 7 is a sample calculation in 2D cylindrical geometry with Comp B as the energetic material sliding in a steel tube. Each frame represents the right side of a cylindrically symmetric system at the times given. The initial velocity of the Comp B is 200 m/s with a coefficient of friction of .2 at the interface. Resolution of the calculation is relatively poor but does provide sufficient evidence of the effect upon

As can be seen, a layer of material is internal energy of the sliding interface. sheared at the interface causing a significant increase in localized internal energy. It should be noted that in the IPFT, shear displacement is minimized by providing an impermeable aft interface. For this calculation, no restraining force was provided (at either surface) which would normally result in a high internal pressure (as occurs in the IPFT).

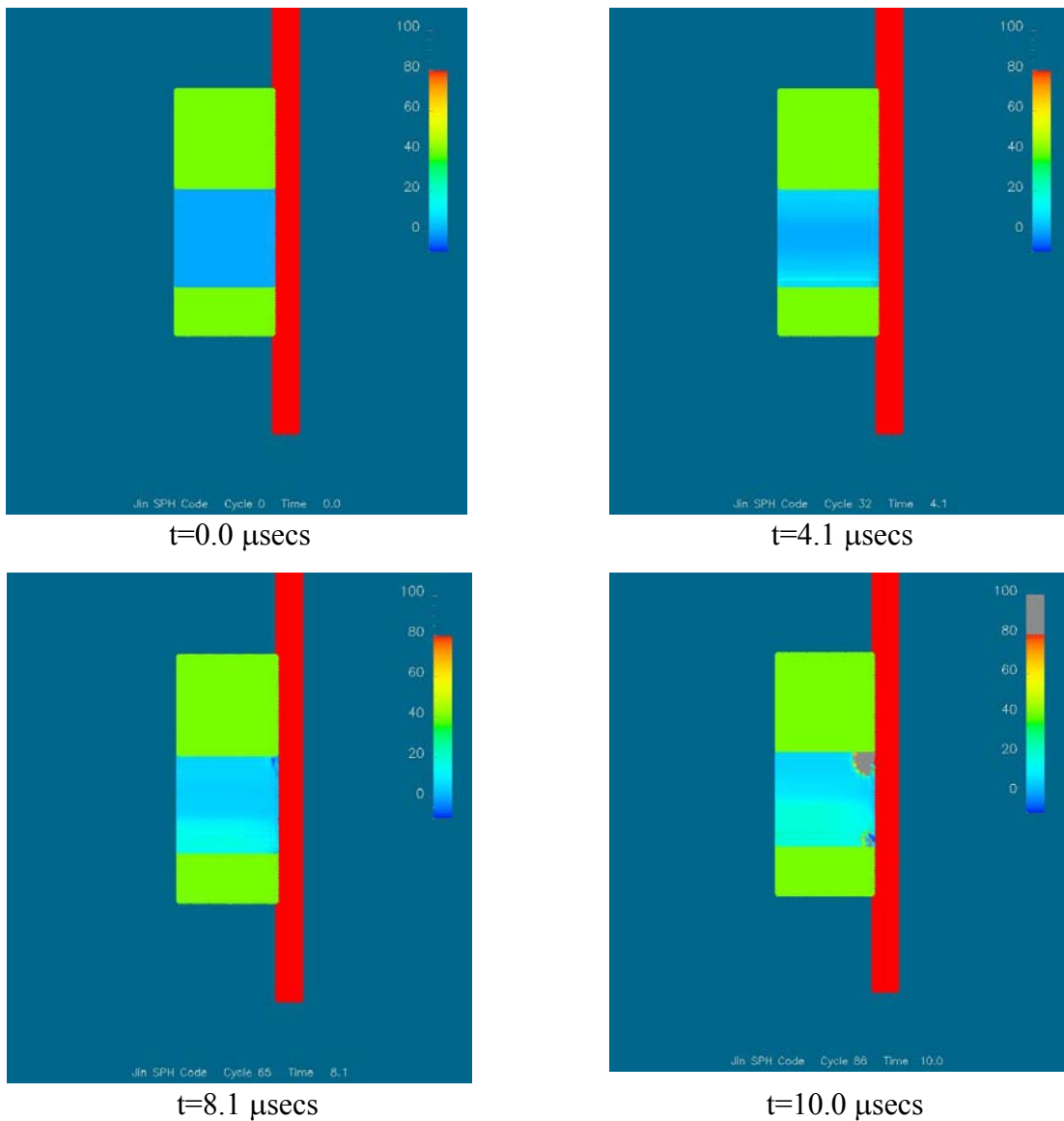


Figure 8. Response of Energetic Material to IPFT Environment-Initial Studies

Figure 8 is a more representative calculation of the environment to which an energetic material is subjected to in the IPFT. The energetic material is given an initial sliding velocity of 20 m/s and a restraining pressure of 1.5 kb. Again, the calculation is performed in 2D axisymmetric coordinates. Three materials, the energetic material (blue), filler E pusher plates (green) and the steel tube (red) are represented. A high stress concentration factor is developed at the corners (explosive, plate, tube interface). After a short incubation period (8  $\mu$ secs), the explosive initiates at the upper right corner. By 10  $\mu$ secs, a burn has developed at the upper right hand corner and an initiation point has developed at the lower right hand corner. Clearly, the time scale is not the same as that previously indicated in the experimental section. However, as of this writing, insufficient data exists (for Cast Cure Explosive A) to develop the appropriate reactive material property parameters for the current Greek Fire model.

## SUMMARY

AFRL/MNME has developed a process, referred to as the Explosive Survivability Protocol, whereby the effect of a low pressure, long impulse load on an explosive material can be determined, primarily with regard to friction initiation. The protocol consists of both experimental and analytical tools, which provide the explosive formulator/user with information regarding the response of the energetic to varying load environments. In general, the constitutive data for the explosive is obtained through use of the piston test. This data, along with anticipated loading profiles, determines the boundary

conditions that the explosive material is subjected to in the IPFT. As a result, both the expected loading profile as well as a factor of safety, can be examined. The effect of friction can be investigated by modifying the surface roughness of the cylinder. Data from the breakaway test as well as friction coefficient information is then used both in modeling as well as application of the material.

## CONCLUSIONS

The results of the IPFT data with respect to Cast Cure Explosive A clearly demonstrate that the IPFT test provides repeatable data regarding friction initiation in the bulk. Previous work has demonstrated that, while the process is conceptually a continuum one, evidence for crystal fracturing under these shear loads is highly likely. As a result, various approaches are underway to model the event including both continuum and microstructural methods. Through the development of a repeatable test, these efforts are expected to be fruitful.

## REFERENCES

1. Field J.E., Swallowe G.M., Heavens S.N., 'Ignition Mechanisms of Explosives During Mechanical Deformation', Proc R Soc. Lond. A 382, 231-244 (1982)
2. Chaudhri M. M., 'The Initiation of Fast Decomposition in Solid Explosives by Fracture, Plastic Flow, Friction, and Collapsing Voids', preprints 9<sup>th</sup> Symposium (International) on Detonation, Portland Oregon (1989)

3. Field J.E., et. al., 'Deformation and Explosive Properties of HMX Powders and Polymer Bonded Explosives', 9<sup>th</sup> Symposium on Detonation, Portland Oregon 1989
4. Foster J.C., Glenn J.G., Hull L.H., Gunger M.E., Galloway M.A., 'Low Pressure Equation of State Measurements for Explosives Using Piston Test', 11<sup>th</sup> Symposium on Detonation, Snowmass Colorado 1998
5. Dienes J. K. 'A Unified Theory of Flow, Hot Spots, and Fragmentation with an Application to Explosive Sensitivity', High Pressure Shock Compression of Solids II, Springer-Verlag (1996)
6. Bowden F. P., Yoffe A. D., 'Initiation and Growth of Explosion in Liquids and Solids', Cambridge University Press, (1952)
7. Armstrong R. W., Coffey C. S., DeVost V. F., Elban W. L., 'Crystal Size Dependence for Impact Ignition of Cyclotrimethylenetrinitramine Explosive' J. Appl. Phys 68 (3) (1990)
8. Matuska D.A., Gunger M.E., 'An Explicitly Porous Model of Heterogeneous Explosive Initiation', Insensitive Munitions & Energetic Materials Technology Symposium, 1998.
9. Dilts G. A. " Moving Least Squares Particle Hydrodynamics -- I. Consistency and Stability", *Int. J. Numer. Mech. Eng.* **44**, 1115-1155 (1999).
10. Dilts G. A. " Moving Least Squares Particle Hydrodynamics -- II", *Int. J. Numer. Meth. Eng.* **48**, 1503-1524 (2000).